HHS Public Access

Author manuscript

Cell Rep. Author manuscript; available in PMC 2017 February 21.

Published in final edited form as:

Cell Rep. 2016 September 20; 16(12): 3260–3272. doi:10.1016/j.celrep.2016.07.052.

iNKT Cell Emigration out of the Lung Vasculature Requires Neutrophils and Monocyte-Derived Dendritic Cells in Inflammation

A Thanabalasuriar[1,3], **A.S Neupane**[1,3], **J Wang**[1,3], **M.F Krummel**[4], and **P Kubes**[1,2,3,*]

[1]Department of Physiology and Pharmacology, University of Calgary, Calgary, AB, Canada T2N 4N1

[2]Department of Microbiology and Infectious Diseases, University of Calgary, Calgary, AB, Canada T2N 4N1

[3]Calvin, Phoebe, and Joan Snyder Institute for Chronic Diseases, University of Calgary, Calgary, AB, Canada T2N 4N1

[4]Department of Pathology, University of California, San Francisco, San Francisco, CA, USA 94110

Abstract

iNKT cells are a subset of innate T cells that recognize glycolipids presented on CD1d molecules and protect against a variety of bacterial infections including S. pneumoniae. Using lung intravital imaging, we examined the behavior and mechanism of pulmonary iNKT cell activation in response to the potent iNKT cell ligand α-galactosylceramide or during *S. pneumoniae* infection. In untreated mice the major fraction of iNKT cells resided in the vasculature, but a small critical population resided in the extravascular space in proximity to monocyte-derived DCs. Administration of either α-GalCer or *S. pneumoniae*, induced CD1d dependent rapid recruitment of neutrophils out of the vasculature. This neutrophil exodus paved the way for extravasation of iNKT cells from the lung vasculature via CCL17. Depletion of monocyte-derived DCs abrogated both the neutrophil and subsequent iNKT cell extravasation. Moreover, impairing iNKT cell migration out of the lung vasculature by blocking CCL17 greatly increased susceptibility to S. pneumoniae infection, suggesting a critical role for the secondary wave of iNKT cells in host defense.

Introduction

Invariant Natural Killer T (iNKT) cells are innate-like immune cells capable of robustly producing a variety of cytokines and anti-microbial molecules (Gao and Williams, 2015) allowing these cells to bridge the gap between innate and adaptive immunity. Subsets of iNKT cells have been identified- NKT1, NKT2 and NKT17, based on the types of cytokines

*Correspondence: pkubes@ucalgary.ca.

Author Contributions: A.T. designed and performed experiments, analyzed data, and wrote the manuscript; A.S.N. performed experiments, analyzed data, and wrote the manuscript; J.W. performed experiments, provided input for interpretation, and edited the manuscript; M.F.K. provided technical advice; and P.K. conceptualized and directed the study, analyzed data, and wrote the manuscript.

they produce in response to lipid antigens such as the prototypical α-galactosylceramide (α-Galcer) (Lee et al., 2015). Strategic localization of these cells matters. Using an immunohistochemistry approach, Lee et al., (2015) demonstrated that different percentages of iNKT cell subpopulations were found in different parts of individual organs such as spleen; NKT1 cells localized preferentially in the red pulp of the spleen, whereas NKT2 cells were in the T cell zone of the white pulp. Administration of α-GalCer intravenously (i.v.) activated the intravascular iNKT cells more readily than the parenchymal iNKT cells of the spleen, highlighting the importance of spatial arrangement (Lee et al., 2015).

There is a growing body of evidence that suggests iNKT cell distribution is also unique in each organ and closely correlated with function. For example, in the liver, iNKT cells reside in the vasculature and patrol the sinusoids. In this way they can sample local changes within blood vessels as well as interact with intravascular liver macrophages known as Kupffer cells. Kupffer cells have a remarkable ability to catch bacteria from the mainstream of blood and then present glycolipids derived from these pathogens to the patrolling iNKT cells. This induces iNKT cells to arrest movement (a hallmark of activation) and begin producing interferon-γ to help drive inflammation (Lee et al., 2010). However, their localization in the blood may also reflect their ability to detect distant organ injury and rapidly alter whole body immunity status. For example, induction of stroke led to the release of molecules that were rapidly detected by intravascular iNKT cells leading to cessation of cell movement and the production of IL10. This led to the dampening of whole body inflammation and an increased susceptibility to infection (Wong et al., 2011). Unlike the liver, iNKT cells did not patrol the blood vessels of joints (Lee et al., 2014). Instead, iNKT cells were strategically localized extravascularly along the length of the few blood vessels within the joint (Lee et al., 2014). Upon infection with *Borrelia burgdorferi,* which adhered to the joint vasculature, iNKT cells were able to recognize and directly kill this pathogen and prevent infection (Lee et al., 2014). Interestingly, in the liver, iNKT cells reside inside the vasculature while in the joints they reside outside and upon stimulation, their compartmentalization does not change (Lee et al., 2010; Lee et al., 2014)

To date, very little is known about the behavior and localization of iNKT cells in the lungs despite their importance in numerous pulmonary diseases. Antibody mediated *in vivo* labeling followed by rapid isolation of cells from whole organs gives values for intravascular versus parenchymal distribution of iNKT cells (Scanlon et al., 2011; Lee et al., 2015). Using this approach with histocytometry, the lung parenchyma appears to mostly harbor NKT17 cells, whereas the blood compartment of the lung contains NKT1 cells (Lee et al., 2015). In another study of explanted lung, Bendelac and colleagues (Scanlon et al., 2011) reported that some iNKT cells were in the vasculature while the remainder were likely in the parenchyma. The limitation of non-live cell imaging techniques is that they fail to capture the migrational dynamics of iNKT cells in tissues. However, live cell imaging of the lung is complicated by several factors such as its relative inaccessibility and the gross movement of the organ. It is not surprising then that there is a dearth of information describing the distribution, behavior, migrational dynamics, and specialized functions of pulmonary iNKT cells. In addition to iNKT cells, there is a resident population of intravascular neutrophils in the lungs (Kreisel et al., 2010). Since both neutrophils and iNKT cells play critical roles in the lung under situations of *S. pneumoniae* infection, imaging could also unveil potential interactions or

relationships between these cell types (Joyce and Van Kaer, 2008). In addition to protecting the lung from *S. pneumoniae* infection, these cells may sense self-antigen and contribute to animal models of asthma and fibrotic disease. (Kim et al., 2005; Paget and Trottein, 2013).

The lung is in constant contact with the outside environment via the airways, allowing environmental particulates and pathogens an easy access to the pulmonary tissue. Pulmonary macrophages housed inside the alveoli are the first line of defense against bacterial dissemination. When pathogens enter the interstitium, interstitial sentinel cells of unknown origin could potentially recruit immune cells from the vasculature to prevent further invasion. However, this interstitial space that separates the aveoli and the capillaries is only a few microns in thickness permitting effective oxygen transport into the blood stream. Any infection that reaches the interstitial space must be rapidly eradicated without excessive inflammation and edema so oxygen transport can continue.

Recent work using two-photon microscopy has allowed visualization of the behavior of immune cells in the lung (Looney et al., 2011; Bose et al., 2015). In this study, we imaged the pulmonary vasculature surrounding the alveoli using a multichannel spinning disk confocal microscope (IVM) which permitted visualization of rapidly occurring events in blood. We carefully examined the behavior of iNKT cells within and outside the vasculature under basal conditions. We found a population of iNKT cells and monocyte-derived DCs in close proximity in the interstitium and observed an almost immediate neutrophil recruitment response to the prototype antigen for iNKT cells, α-GalCer. These neutrophils functioned as trailblazers for the large intravascular iNKT cell population, helping them extravasate into the lung interstitial space in a CCL17 dependent manner. Lastly, we used a bona fide *Streptococcus pneumoniae* infection model to demonstrate that the same progression of events seen with α-Galcer administration, also occurred in response to this pathogen. Impairing iNKT cell migration out of the lung vasculature by blocking CCL17 greatly increased susceptibility to *S. pneumoniae* infection, suggesting a critical role for the secondary wave of iNKT cells ensuring survival during *S. pneumoniae* infection.

Results

iNKT cells reside in both the lung vasculature and the lung interstitial parenchyma

Using an intravital microscope and positioning a small window with gentle suction on an otherwise normally respiring lung of a live anesthetized mouse so that it could be visualized over extended periods of time *in vivo* without motion artifacts (Looney et al., 2011). The lung continued to be perfused with air, and the blood within the vasculature continued to flow around the alveoli (Movie S1). Importantly, platelet aggregation and adhesion, a hallmark of inflammation and endothelial activation, was not seen in the lung vasculature during basal imaging sessions (data not shown). Our initial visualization of the pulmonary vasculature revealed a very dynamic environment with extremely dense microvasculature with many overlapping vessels.

To date the best tool to visualize iNKT cells *in vivo* is by using a CXCR6^{GFP+} transgenic mouse (Scanlon et al., 2011; Wong et al., 2011). Using whole mount staining techniques we found that the brightest green cells per field of view (FOV) were also PBS-57 loaded CD1d

tetramer (referred to from hereon as “tetramer”) positive iNKT cells. In a 20x FOV, 60–70% of CXCR6^{GFP+} cells were tetramer positive iNKT cells (Figure S1). Using IVM we found that the lung had ample CXCR6^{GFP+} iNKT cells inside very fast flowing capillaries (Movie S1).

Many of the iNKT cells were observed in the blood stream as 1) they conformed to the size of the capillaries, 2) they often suddenly appeared (tethering to endothelium from mainstream of blood), 3) the majority of crawling and adherent iNKT cells were often rapidly displaced some distance due to high shear in the blood vessels and 4) would rapidly disappear as they detached from the vessel wall and re-entered the mainstream of blood (Figure 1A; Movies S2,3,4). A 3-D reconstruction clearly supported the notion that the majority of iNKT cells were intravascular (Movie S5). Extensive, detailed behavioural examination of the iNKT cells revealed that approximately 40% of cells tethered, 20% crawled and the remaining 40% were stationary (Figure 1B). Two approaches were taken to identify the frequency of the cells that were intravascular versus extravascular. We termed the first approach ‘shadowing’ where displacement of TRITC-dextran in the lumen of blood by cells produced an unlit/dark area occupied by the cell. Thus, if a CXCR6^{GFP+} iNKT cell resided in the vasculature, there would be a shadow of the cell visible in the TRITC channel that conformed to the size and shape of the GFP^{+} cell (Figure 1C) (Auffray et al., 2007). Approximately, 75–80% of iNKT cells were in the vasculature (Figure 1D).

The second approach to differentiate the spatial distribution of cells was to use an i.v. infusion of anti-CD45 antibody (a pan leukocyte marker) for a very brief period of time prior to the harvest of tissues. This technique only labels cells within the vasculature (Barletta et al., 2012); the lungs were then harvested for flow cytometric analysis. Almost all neutrophils were labeled with anti-CD45, while no alveolar macrophages were labeled (data not shown). This confirmed that only vascular but not tissue resident immune cells were labeled with this technique. When quantifying the distribution of iNKT cells (identified using CD1d tetramer staining), we observed that 80% of cells were labeled with anti-CD45 and 20% were protected from labeling (Figure 1E), further corroborating our intravital imaging data.

Pulmonary iNKT cells migrate into the lung interstitium upon activation

Intravenous administration of α-GalCer resulted in dramatic changes to the behavior and phenotype of pulmonary iNKT cells. At 3 hours post i.v. administration of α-Galcer, the majority of iNKT cells crawled persistently for long lengths and very few were observed to tether (Figure 1B). Unexpectedly, from this time point on up until 24 hours iNKT cells began crossing the vascular barrier and moved into the extravascular space where they appeared much more flattened and larger in size (Figure 1D). Very few iNKT cells were found in the bronchial lavage (BAL) fluid (discussed later). The increased appearance in size is reflective of these cells being in the very narrow (1–3 um) interstitial space between the vasculature and the alveoli. By 24 hours, approximately three quarters of the iNKT cells had extravasated into the interstitium, as assessed with the shadowing technique (Figure 1D). Extravasating iNKT cells also upregulated the surface expression of CD69, an early activation marker (Figure 1F). Using the i.v. anti-CD45 infusion approach, we confirmed that indeed 80% of pulmonary iNKT cells had extravasated out of the vasculature (Figure

1E). Once in the intersitium the cells became relatively stationary; they showed some movement but very little displacement (Movie S6A). Interestingly, only tetramer positive CXCR6^{GFP+} cells (iNKT cells) crossed into the intersitium after α-Galcer administration while the tetramer negative (non-iNKT) cells did not respond to α-Galcer administration (Figure S2).

Since many pathogens enter the lung via the intratracheal route, we next administered the α-GalCer via this route. Under these conditions, the iNKT cell behavior was nearly identical to i.v. α-Galcer, with approximately 80% of cells leaving the vasculature and moving into the intersitium (Figure 2A,B; Movie S6A,B). However despite the intratracheal route of α-Galcer administration very few iNKT cells migrated into the airspaces, confirmed by flow cytometric analysis of BAL fluid (Figure 2D), indicating that these cells were retained predominately in the lung interstitial space. We used 3D modeling of lung whole mount and found that again, the iNKT cells clustered and sat just above the vascular bed in the interstitial space (Figure 2C). The migration of iNKT cells occurred about 10 hours later when α-Galcer was administered intratracheally versus intravenously. This delay likely reflects the difference in time that was required for α-Galcer to cross the much tighter epithelial barrier in airways and aveoli. From these data we concluded that pulmonary iNKT cell dynamics were similar whether the stimulus was given intratracheally or intravenously and we therefore used i.v. administration of α-Galcer to assess the dynamics of iNKT cell activation.

Neutrophils play an important role in iNKT cell extravasation

Unexpectedly, i.v. administration of α-Galcer resulted in a robust influx of neutrophils into the lung as early as 30 minutes, peaking at 2 hours, and stabilizing back to normal by 24 hours (Figure 3A). This did not occur in other organs such as spleen (Figure 3A). Moreover, the recruited neutrophils rapidly moved out of the vasculature into the interstitium and onwards into the alveoli (Figure 3B and data not shown). Intravenous administration of α-Galcer to CD1dKO mice did not result in increased recruitment of neutrophils, demonstrating that this was a CD1d dependent event (iNKT cells in interstitium interacting with CD1d presenting cells) and not an artifact of LPS or other neutrophil stimulant contamination (Figure 3C). Similar recruitment of neutrophils could also be observed when α-GalCer was given intratracheally (Figure S3).

To determine the role of neutrophils in changing iNKT cell behavior, we utilized antibody-mediated depletion of neutrophils. It is worth noting that this approach did not affect the monocyte population in the lung (data not shown). Surprisingly, in mice depleted of neutrophils, iNKT cell extravasation was significantly impaired as assessed using IVM shadowing and flow cytometry (Figure 3E and F). As seen in figure 3D, there were fewer large flattened iNKT cells (characteristic of interstitial location) observed outside the vasculature in neutrophil depleted mice. Indeed, most iNKT cells displayed shadows in TRITC-dextran stained blood vessels. Moreover, neutrophil depletion led to impairment in iNKT cell activation after α-Galcer administration (Figure 3G). However there were still some iNKT cells activated, presumably those that were already in the interstitium. We

concluded from this data that iNKT cell extravasation and activation was at least partly dependent on the neutrophils guiding the iNKT cells into the interstitium.

We further assessed whether neutrophil activation alone could induce iNKT cell extravasation. Intratracheal administration of neutrophil specific chemokine KC (200ng) resulted in a marked increase in neutrophil extravasation (Figure 4A and 4B). Interestingly, administration of KC alone also resulted in extravasation of iNKT cells despite the fact that iNKT cells did not express receptors for KC (Figure S4). Approximately three quarters of $CXCR6^{GFP+}$ cells migrated into the interstitium after KC, as assessed by the shadowing technique (Figure 4A). We used flow cytometry to confirm that the extravasated $CXCR6^{GFP+}$ cells were in fact iNKT cells (Figure 4C). Unlike with α-Galcer treatment, KC administration resulted in only a modest increase in CD69 expression on iNKT cells (Figure 4D). Clearly, activated neutrophils could induce iNKT cell extravasation but a CD1d dependent glycolipid is required for overt activation of iNKT cells.

The chemokine CCL17 is important for iNKT cell extravasation

Next we systematically examined which molecules were responsible for guiding iNKT cells out of the vasculature in response to α-GalCer treatment. Blocking GPCR with pertussis toxin prevented iNKT extravasation after α-Galcer, suggesting that chemokines were likely involved (Figure 4E). Chemokine receptors CXCR3, CXCR6 and CCR4 have all been shown to mediate iNKT cell chemotaxis (Thomas et al., 2003). Blocking CXCR3 or neutralizing its ligand MIG had little to no effect on iNKT cell migration out of the vasculature in response to α-Galcer treatment (Figure 4F and MIG data not shown). CXCR6 deficiency also failed to inhibit emigration of iNKT cells out of the vasculature (data not shown). To inhibit CCR4 we blocked the ligand CCL17 and found complete inhibition of iNKT cell emigration in response to α-GalCer treatment (Figure 4F). Blocking CCL17 also inhibited KC induced neutrophil dependent iNKT cell extravasation (Figure 4B). These data supported the idea that neutrophils mediate the extravasation of iNKT cells from the vasculature by potentially stimulating the release of CCL17.

Monocyte derived dendritic cells in the lung are able to present antigen to iNKT cells

While neutrophils imparted a crucial role in iNKT cell extravasation, there was a lack of iNKT-neutrophil interactions using our imaging (data not shown). Therefore, it was unlikely that neutrophils presented antigen to iNKT cells. We hypothesized that antigen-presenting cells (APCs) existed in the lung interstitium which were crucial for both the early and late iNKT cell activation. We used fluorescently labeled β–Galcer, an α-Galcer derivative, to identify these APCs (Arora et al., 2014). 12–18 hours after treatment, a population of cells which bound the β–Galcer were visualized. This strategy does not accurately reflect when the cells start binding β-Galcer (presumably much earlier than 12 hours) but rather which cells bound and accumulated most of the antigen. The β-Galcer binding cells were observed outside the vasculature (Figure 5A and C), and their shape and size closely resembled that of $CD11c^{+}$ DC in the lungs (Figure 5B). These extravascular cells actively sampled the capillaries using their pseudopods and interacted with antigenic particles from the blood stream (Movie S7). These cells were identified as $CD103^{-}$ $CD11c^{+}$ $MHCII^{hi}$ DCs (Table

S1). The cells also expressed Ly6C, Mar1 and CD64 suggesting a monocytic origin (Table S1) (Plantinga et al., 2013; Jakubzick et al., 2008).

We next addressed the importance of these DCs in iNKT cell activation and extravasation. Complete ablation of circulating monocytes and DCs by administering Chlodronate loaded liposomes (CLL) and diphtheria toxin (DT), respectively, to CD11c-DTR mice depleted all detectable DCs in the interstitium and abrogated activation and extravasation of pulmonary iNKT cells, and reduced recruitment of neutrophils into the lung (Figure 5D, E, and F). It is worth mentioning that $CCR2^{hi}$ monocytes are capable of differentiating into pulmonary DCs and *ccr2*−/− mice (CCR2KO) have an impairment in dendritic cell maturation and activation ((Jakubzick et al., 2008); Chiu et al., 2004). However, iNKT cell activation and neutrophil recruitment was intact in CCR2KO mice (Figure S5A–5B). This might be expected since another set of CD103 negative, CD11b high monocyte-derived DCs have been identified in lungs which do not require CCR2 for migration (Jakubzick et al., 2008).

iNKT cell extravasation is important in *S. pneumoniae* infections

S. pneumoniae is a clinically important Gram-positive respiratory pathogen which is capable of causing severe disease in humans. It has recently been shown that *S. pneumoniae* harbors an iNKT cell specific glycolipid on its cell surface and mice lacking iNKT cells are far more susceptible to this infection (Kinjo et al., 2011). Thus, we asked how iNKT cells would behave upon infection with this complex pathogen. Intratracheal infection with *S. pneumoniae* resulted in changes to iNKT cell behavior similar to that observed after α-Galcer administration. Twenty-four hours post-infection, iNKT cells predominantly crawled and by 48 hours were mostly stationary (Figure 6A). We confirmed that these cells had migrated into the interstitium using IVM shadowing and *in vivo* anti-CD45 labeling techniques (Figure 6B and C). iNKT cells extravasated at 48 hours post *S. pneumoniae* infection as opposed to 24 hours with α-Galcer (Figure 6B and 6C). These data suggest similar response of iNKT cells to α-Galcer treatment and *S. pneumoniae* infection, albeit with a delayed response to the pathogen.

Mice that lacked iNKT cells were highly susceptible to *S. pneumoniae* infection (Kawakami et al., 2003) (Figure 6D) as were mice deficient in neutrophils (data not shown). To test whether the increased mortality was due to the wave of iNKT cells following neutrophils into the infected mice, we blocked iNKT cell extravasation by blocking CCL17, in mice infected with *S. pneumoniae.* Although neutrophils still migrated into the lungs, presumably via pathogen associated molecular patterns and other stimuli associated with a complex infection, iNKT cells no longer followed when CCL17 was blocked (data not shown). A very similar increase in mortality was observed when CC17 was blocked in mice as when mice lacked iNKT cells (Figure 6D). This indicated that extravasation of iNKT cells out of the vasculature is crucial for survival and mounting an effective immune response against pulmonary infection with *S. pneumoniae*.

Discussion

In this study we analyzed the behavior and mechanisms of activation of pulmonary iNKT cells using intravital microscopy. *In vivo* imaging provided us with significant insight into

iNKT cell response in the lung. There was a striking and distinct behavior of pulmonary iNKT cells versus those in other organs in response to either a CD1d antigen or an infectious agent like *S. pneumonia*e. In the lung under basal conditions, iNKT cells predominately reside in the vasculature, while a small population reside in the interstitium. Upon activation, pulmonary iNKT cells migrated out of the vasculature into the interstitium. This behaviour is considerably different from what has been observed in other organs. Interestingly, neutrophils guide the iNKT cells into the interstitial space and while the neutrophils continue into the alveoli, the iNKT cells arrest as they come into contact with antigen presenting cells, including monocyte-derived dendritic cells. Very few if any iNKT cells ever migrated into the airways. We found that the $CD11c^+$ monocyte derived DCs and perhaps other subtypes of DCs were the main antigen presenting cells in the lung based on their ability to effectively take up the reporter β-Galcer. In the absence of these DCs, neutrophil and iNKT cell activation and recruitment into the interstitium was severely hindered. The net effect of this well-choreographed process involving multiple immune cell types is that infections like *S. pneumoniae* are effectively dealt with. However, the interruption of any of these processes leads to increased mortality.

Our working model shown in Figure 7 is that upon administration of either α-Galcer or *S. pneumoniae,* a CD1d bearing DC in the interstitium presents a glycolipid antigen to interstitial iNKT cells and this leads to rapid recruitment of neutrophils into the interstitium. Neutrophils guide iNKT cells from the vasculature into the interstitium via CCL17. Although the major population of iNKT cells resides in the vasculature, it is critical to note that there is a smaller population of iNKT cells, a pioneer iNKT cell, in the tissue under basal conditions. These cells have been reported as primarily an IL17 producing subset (Lee et al., 2015). Activation of the Th17 arm of immunity potently induces neutrophil recruitment (Liang et al., 2007). Although there is presently no way of dissociating the functions of the tissue and vascular iNKT cell populations, the fact the neutrophil recruitment began as early as 30 min and was dependent upon CD1d strongly supports a role for interstitial cells. In fact, these pioneer iNKT cells may function as the sentinel immune cells for *S. pneumoniae*, and may explain why iNKT cell deficient mice die as quickly as neutrophil deficient mice. Whether extravascular iNKT cells or DCs are the source of the neutrophil chemoattractants was not investigated in this study. However, a companion paper by Xu et al. (2015) explored the complex dynamic interplay and two way cross-talk between these cells. The authors identified that the neutrophil recruitment could be induced by 1) the iNKT-DC interaction and the DCs were the source of the chemoattractant, and 2) that prostaglandins were the neutrophil chemoattractant involved. There is a striking similarity in cell types and mechanisms of action described using *in vitro* human systems by Xu et al., and our own *in vivo* data in the mouse lung.

While infections in liver caused iNKT cells to become activated, no emigration out of the liver vasculature was ever noted. In the spleen, in response to *S. pneumoniae*, King et al., (2011) identified iNKT cells migrating long distances to the marginal zone to help with effector functions including eradication of *S. pneumonia*e in this organ. Finally, in joints (Lee et al., 2014) and intestine (unpublished), we found that iNKT cells are already located outside the vasculature, and, in the former they tend to abut the blood vessels, keeping pathogens from infiltrating into this tissue. However, in none of these organs have we

observed migration of iNKT cells out of the vasculature in response to pathogens. It is intriguing that the iNKT cells were not able to emigrate out of the vasculature in the absence of neutrophils. In fact, we identified that neutrophils were critical for guiding iNKT cells across the endothelium and into the interstitial space. The mechanism by which this occurs makes use of CCL17, a molecule previously reported to be important to induce iNKT cell chemotaxis. In a previous study of airway hyper-responsiveness (AHR), mice deficient for CCR4 (CCL17 receptor) did not develop AHR (Meyer et al., 2007). The group concluded that the CCR4 receptor on iNKT cells was important for their localization in the lung (Meyer et al., 2007). Our study extends this observation to highlight the crucial role of CCR4/CCL17 axis in iNKT cell emigration into the interstitium in response to infections.

There appears to be an inherent trait of emigrating neutrophils to recruit iNKT cells; a single neutrophil specific chemokine (KC) with no other stimulus was sufficient to induce iNKT cells to follow the neutrophils out of the vasculature. Recently, it has been reported that during influenza infections, neutrophils appeared to guide CD8 T cells into airways via trails of CXCL12 present on their elongated uropods. (Lim et al., 2015). Although we have similarly noticed these long tails form across the endothelial barrier, potentially suggesting a similar mechanism of action, the importance of these tails relative to release of soluble chemokines remains to be determined. Interestingly, while the neutrophils continued emigration past the interstitium and onwards to the alveoli, the iNKT cells remained in the very small space between the endothelium of the capillaries and epithelium of the alveoli (Figure 2D and data not shown). Using β-Galcer we identified that the most prominent antigen presenting cells were localized in the interstitium and presumably bound the iNKT cells, over-riding any further follow-me signals from the neutrophils.

Our intravital data would suggest that while these monocyte-derived DCs were in an extravascular position, they are able to extend their processes into the blood stream and sample for antigens (Movie S7). This may explain why i.v. administration of α-Galcer could activate interstitial iNKT cells in less than 30 min to induce very rapid neutrophil recruitment. While elaborate, this would be a very elegant way of detecting pathogens and noxious stimuli and respond immediately to such dangers that are systemic or airborne. Moreover, a chemokine gradient into the interstitium could be set up via an interstitial cell. Since the lung is such an essential organ which ensures adequate oxygenation of blood across the pulmonary interstitial space, this mechanism of sampling in blood could induce rapid and immediate eradication of any potential pathogenic threat minimizing further inflammation and would be essential for survival.

In this study, we have established that iNKT cells can cross the vasculature in response to activation. This behaviour was very specific for pulmonary iNKT cells. We identify that neutrophils are critical for guiding the iNKT cells, perhaps because neutrophils have the proteases necessary for breaching this barrier. We also identify the molecule that functions as a guidance cue, namely the chemokine CCL17. Blocking this chemokine prevented iNKT cell extravasation, leading to increased mortality in an infection model. The fact that even a generic neutrophil chemokine, KC, resulted in the extravasation of iNKT cells raises the possibility that in some inappropriate lung inflammatory processes such as asthma, COPD

and fibrosis, blocking CCL17 could resolve or reduce the ongoing inflammation and provide some therapeutic benefit.

Methods

Mice. 6–8 week old C57BL/6 (B6), *CD1d*−/− (CD1dKO), *Jα18*−/− (Jα18KO), *cd11c-DTR* (CD11c-DTR), CD11c-EYFP (CD11c-YFP), *ccr2*−/− (CCR2KO), and B6.CXCR6-GFP knock-in ($CXCR6^{GFP+}$) were purchased from the Jackson Laboratory. All mice were housed under specific pathogen-free, double-barrier unit at the University of Calgary. Mice were fed autoclaved rodent feed and water *ad libitum*. All protocols used were in accordance with the guidelines drafted by the University of Calgary Animal Care Committee and the Canadian Council on the Use of Laboratory Animals.

Intravital microscopy (IVM). Multichannel spinning-disk confocal intravital microscope was used to image mouse lungs. The set up was adapted from previously described work (Looney et al., 2011). Briefly, Mice were anaesthetized (10 mg/Kg xylazine hydrochloride and 200 mg/Kg ketamine hydrochloride) and the body temperature maintained at 37°C using a heating pad (CU-201, Live Cell Instruments). The right jugular vein was cannulated to administer fluorescent dyes and additional anesthetic. The trachea of the mouse is exposed and a small catheter was threaded into the trachea. The catheter was then attached to a small rodent ventilator (Harvard Apparatus). The mouse was placed on its right lateral decubitus position and three ribs were removed in order to expose the lung. The lung was stabilized with a small suction chamber as described (Looney et al., 2011). Images were acquired with an upright microscope (BX51; Olympus) using a 20x/0.95W NA water dipping XLUM Plan F1 objective (Olympus). The microscope was equipped with a confocal light path (WaveFx, Quorum) based on a modified Yokogawa CSU-10 head (Yokogawa Electric). A 512 x 512 pixel back-thinned electron multiplying charge-coupled device camera (C9100-13, Hamamatsu) was used for fluorescence detection. Simultaneous behavior of multiple cell types in the lung was assessed using three (488, 561, and 635-nm) laser excitation wavelengths (Cobalt, Stockholm, Sweden) in rapid succession and visualized with the appropriate long-pass filters (Semrock, Rochester, NY). Volocity software (PerkinElmer) was used to acquire and analyze images (Wong et al., 2011; McDonald et al., 2010).

In vivo labeling for IVM. Anesthetized mice were given fluorescently labeled antibodies (below) and/or TRITC-dextran (Life Technologies) i.v. via the jugular vein prior to imaging. Neutrophils were identified with 2μg of AF647 conjugated Ly6G, clone 1A8 (eBioscience); the vasculature was identified with 2μg of PE labeled CD31 (PECAM-1, eBioscience). For shadowing experiments, 100μL of TRITC-dextran was administered.

In vivo labeling of APC. C11 TopFluor® Galactosyl Ceramide N-[11-(dipyrromethene boron difluoride)undecanoyl]-D-galactosyl-β1-1′-D-erythro-sphingosine, referred to in the text as "β –gal" was used to identify APCs which captured and presented glycolipids to iNKT cells. β-gal (Avanti) was prepared as previously described (Arora et al., 2014) and was administered i.v. 12–18 hours prior to experiments.

Bacterial growth and infection. *Streptococcus pneumonaie* strain D39 was grown on blood agar plates overnight at 37° C with CO_2. Single colonies were picked from plates and grown for 10–12 hours in BHI broth at 37° C with CO_2, no shaking. Once an OD600 of 0.5 was reached, bacteria were resuspended in PBS and mice were given 30–35μL of suspension (aerosolized) to achieve a dose of $1x10^5$ CFU per mouse.

Aerosolization into mouse airways: Small rodent aerosolization kit was purchased from PenCentury. All animals that were treated via the intratracheal route received 30–35μL of aerosolized compounds. Mice were aerosolized with 200ng of CLL17 (R&D Systems) or KC (R&D Systems), 400ng of α-Galcer (Kirin Brewery), and 1–3 $x10^5$ CFUs of *S. pneumoniae*. Aerosolized saline (30–35μL) was used for control in mice that we labeled untreated.

In vivo labeling of vascular leukocytes for flow cytometry. Mice were anesthetized with Ketamine and xylazine (200 mg/Kg and 10 mg/Kg, respectively). 3μg of PE-Cy7 labeled anti-CD45 (eBioscience) was injected in a total volume 150–200μL of sterile saline intravenously (i.v) via the tail vein or the retro-orbital venous plexus. Body temperature was maintained at 37°C. Mice were sacrificed 10 minutes after i.v. administration of the antibody. The lung was exsanguinated by perfusing cold PBS from the right ventricle and then harvested for flow cytometric analysis. Lung digestion for *in vivo* labeling experiments was performed using digestion buffer- PBS with 1mg/ml collagenase Type X1, 60U DNase, and 0.1mg/mL Kunitz-type soybean trypsin inhibitor (Sigma).

Flow Cytometry: Mice were euthanized with CO_2. Lungs were perfused with 10mL of ice cold saline injected through the right ventricle of the heart. Perfused lungs were removed, minced and placed in digestion buffer- PBS with 1mg/ml collagenase Type X1 and 60U DNase (Sigma). Lungs were digested for 30 minutes and passed through a 70μm filter. Residual red blood cells were lysed using ACK (Gibco). The cells were blocked using 2.4G2 (BioXcell) for 30 minutes. Cells were stained for 30 minutes with indicated markers. Cells were stained with PE labeled anti-mouse CD1d (1B1), CD69 (HI.2F3), CD103 (M290), CD205 (205yekta), I-A/I-E (M/114.15.2), PBS-57 loaded or unloaded CD1d tetramer or SiglecF (E50-2440); APC, AlexaFluor 647 or eFluor 660 labeled anti-mouse Ly6G (1A8), SiglecF (E50-2440), CD11c (N418), CD64 (X54-5/7.1), FCeR1 (MAR-1) or PBS-57 loaded or unloaded CD1d tetramer; PerCP-Cy5.5 labeled anti-mouse CD45 (30-F11), CD3e (145-2C11) or Ly6C (HK1.4); PE-Cy7 labeled anti-mouse CD11b (M1/70) or CD45 (30-F11); eFluor 450 labeled anti-mouse CD45R (RA3-6B2); APC-eFluor 780 labeled anti-mouse F4/80 (BM8). All antibodies were from eBioscience, BD or NIH tetramer core, unless indicated otherwise. Samples were run using FACSCanto flow cytometer (BD) and analyzed using FlowJo software (Tree Star). For iNKT cell study cells were gated as shown in Figure S7A. For monocyte derived DCs cell study cells were gated as shown in Figure S7B.

Whole mount staining. Mice were euthanized by overdosing with Ketamine and xylazine then their lungs were inflated using 4% low melting agarose (Invitrogen). Once agarose was cooled lung were sliced into 300μm slices using a vibratome (Leica). Lungs were blocked in PBS + 1% BSA and 2μg FC block (2.4G2) for an hour then stained in a solution of PBS+1%

BSA with a 1:200 dilution of Loaded or unloaded tetramer (NIH tetramer core) for 12–17 hours at 4° Celsius. Samples were washed in PBS+1% BSA 5–10 times and immediately imaged using inverted Nikon A1Rsi confocal microscope.

Depletion experiments. For neutrophil depletion 200μg of anti-GR1 antibody, clone (RB6-8C5) (BioXcell), was administered intraperitoneally, 24 hours prior to experiments. It is important to note that we did not observe depletion in the monocyte population upon administration of anti-GR1 (data not shown). Nevertheless, mice deficient in CCR2 lacking inflammatory monocytes had responses very similar to WT mice. To deplete $CD11c^+$ DCs 80ng of DT was given intraperitoneally, 48 hours prior to experiments to CD11c-DTR mice. Monocytes were depleted with i.v. administration (200μL) of CLL 24 hours before experiments. CD11c-DTR animals were used for DC and monocyte depletion.

Statistical analysis. Statistical analysis was performed using PRISM software (Graphpad). All values are expressed as mean ± SEM. Data were compared using one-way ANOVA with Bonferroni multiple comparisons post hoc test. Survival analysis was assessed using Mantel-Cox test. Statistical significance was accepted at $P < 0.05$.

Supplementary Material

Refer to Web version on PubMed Central for supplementary material.

Acknowledgments

The authors would like to thank Dr. Robert M. Strieter in University of Virginia School of Medicine for providing the CXCR3 polyclonal blocking antibody, Dr. Woo-Yong Lee and Michelle Willson for technical support. This work was supported by the CIHR Post-doctoral Fellowship (A.T.), CIHR Lung Group Grant for Chronic Inflammation (P.K.), CIHR Banting Fellowship (J.W.), and Alberta Innovate Health Solution Doctoral Fellowship (A.S.N.). The authors declare no conflicts of interest.

References

Arora P, Baena A, Yu KO, Saini NK, Kharkwal SS, Goldberg MF, Kunnath-Velayudhan S, Carreno LJ, Venkataswamy MM, Kim J, et al. A single subset of dendritic cells controls the cytokine bias of natural killer T cell responses to diverse glycolipid antigens. Immunity. 2014; 40:105–116. [PubMed: 24412610]

Auffray C, Fogg D, Garfa M, Elain G, Join-Lambert O, Kayal S, Sarnacki S, Cumano A, Lauvau G, Geissmann F. Monitoring of blood vessels and tissues by a population of monocytes with patrolling behavior. Science. 2007; 317:666–670. [PubMed: 17673663]

Barletta KE, Cagnina RE, Wallace KL, Ramos SI, Mehrad B, Linden J. Leukocyte compartments in the mouse lung: distinguishing between marginated, interstitial, and alveolar cells in response to injury. Journal of immunological methods. 2012; 375:100–110. [PubMed: 21996427]

Bose O, Baluk P, Looney MR, Cheng LE, McDonald DM, Caughey GH, Krummel MF. Mast cells present protrusions into blood vessels upon tracheal allergen challenge in mice. PloS one. 2015; 10:e0118513. [PubMed: 25789765]

Gao Y, Williams AP. Role of Innate T Cells in Anti-Bacterial Immunity. Frontiers in immunology. 2015; 6:302. [PubMed: 26124758]

Jakubzick C, Tacke F, Ginhoux F, Wagers AJ, van Rooijen N, Mack M, Merad M, Randolph GJ. Blood monocyte subsets differentially give rise to CD103+ and CD103− pulmonary dendritic cell populations. Journal of immunology. 2008; 180:3019–3027.

Joyce S, Van Kaer L. Lung NKT cell commotion takes your breath away. Nature medicine. 2008; 14:609–610.

Kawakami K, Yamamoto N, Kinjo Y, Miyagi K, Nakasone C, Uezu K, Kinjo T, Nakayama T, Taniguchi M, Saito A. Critical role of Valpha14+ natural killer T cells in the innate phase of host protection against Streptococcus pneumoniae infection. European journal of immunology. 2003; 33:3322–3330. [PubMed: 14635040]

Kim JH, Kim HY, Kim S, Chung JH, Park WS, Chung DH. Natural killer T (NKT) cells attenuate bleomycin-induced pulmonary fibrosis by producing interferon-gamma. The American journal of pathology. 2005; 167:1231–1241. [PubMed: 16251408]

Kinjo Y, Illarionov P, Vela JL, Pei B, Girardi E, Li X, Li Y, Imamura M, Kaneko Y, Okawara A, et al. Invariant natural killer T cells recognize glycolipids from pathogenic Gram-positive bacteria. Nature immunology. 2011; 12:966–974. [PubMed: 21892173]

Kreisel D, Nava RG, Li W, Zinselmeyer BH, Wang B, Lai J, Pless R, Gelman AE, Krupnick AS, Miller MJ. In vivo two-photon imaging reveals monocyte-dependent neutrophil extravasation during pulmonary inflammation. Proceedings of the National Academy of Sciences of the United States of America. 2010; 107:18073–18078. [PubMed: 20923880]

Lee WY, Moriarty TJ, Wong CH, Zhou H, Strieter RM, van Rooijen N, Chaconas G, Kubes P. An intravascular immune response to Borrelia burgdorferi involves Kupffer cells and iNKT cells. Nature immunology. 2010; 11:295–302. [PubMed: 20228796]

Lee WY, Sanz MJ, Wong CH, Hardy PO, Salman-Dilgimen A, Moriarty TJ, Chaconas G, Marques A, Krawetz R, Mody CH, Kubes P. Invariant natural killer T cells act as an extravascular cytotoxic barrier for joint-invading Lyme Borrelia. Proceedings of the National Academy of Sciences of the United States of America. 2014; 111:13936–13941. [PubMed: 25205813]

Lee YJ, Wang H, Starrett GJ, Phuong V, Jameson SC, Hogquist KA. Tissue-Specific Distribution of iNKT Cells Impacts Their Cytokine Response. Immunity. 2015; 43:566–578. [PubMed: 26362265]

Lim K, Hyun YM, Lambert-Emo K, Capece T, Bae S, Miller R, Topham DJ, Kim M. Neutrophil trails guide influenza-specific CD8(+) T cells in the airways. Science. 2015; 349:aaa4352. [PubMed: 26339033]

Looney MR, Thornton EE, Sen D, Lamm WJ, Glenny RW, Krummel MF. Stabilized imaging of immune surveillance in the mouse lung. Nature methods. 2011; 8:91–96. [PubMed: 21151136]

Meyer EH, Wurbel MA, Staton TL, Pichavant M, Kan MJ, Savage PB, DeKruyff RH, Butcher EC, Campbell JJ, Umetsu DT. iNKT cells require CCR4 to localize to the airways and to induce airway hyperreactivity. Journal of immunology. 2007; 179:4661–4671.

Paget C, Trottein F. Role of type 1 natural killer T cells in pulmonary immunity. Mucosal immunology. 2013; 6:1054–1067. [PubMed: 24104457]

Plantinga M, Guilliams M, Vanheerswynghels M, Deswarte K, Branco-Madeira F, Toussaint W, Vanhoutte L, Neyt K, Killeen N, Malissen B, et al. Conventional and monocyte-derived CD11b(+) dendritic cells initiate and maintain T helper 2 cell-mediated immunity to house dust mite allergen. Immunity. 2013; 38:322–335. [PubMed: 23352232]

Scanlon ST, Thomas SY, Ferreira CM, Bai L, Krausz T, Savage PB, Bendelac A. Airborne lipid antigens mobilize resident intravascular NKT cells to induce allergic airway inflammation. The Journal of experimental medicine. 2011; 208:2113–2124. [PubMed: 21930768]

Thomas SY, Hou R, Boyson JE, Means TK, Hess C, Olson DP, Strominger JL, Brenner MB, Gumperz JE, Wilson SB, Luster AD. CD1d-restricted NKT cells express a chemokine receptor profile indicative of Th1-type inflammatory homing cells. Journal of immunology. 2003; 171:2571–2580.

Wilson R, Cohen JM, Jose RJ, de Vogel C, Baxendale H, Brown JS. Protection against Streptococcus pneumoniae lung infection after nasopharyngeal colonization requires both humoral and cellular immune responses. Mucosal immunology. 2015; 8:627–639. [PubMed: 25354319]

Wong CH, Jenne CN, Lee WY, Leger C, Kubes P. Functional innervation of hepatic iNKT cells is immunosuppressive following stroke. Science. 2011; 334:101–105. [PubMed: 21921158]

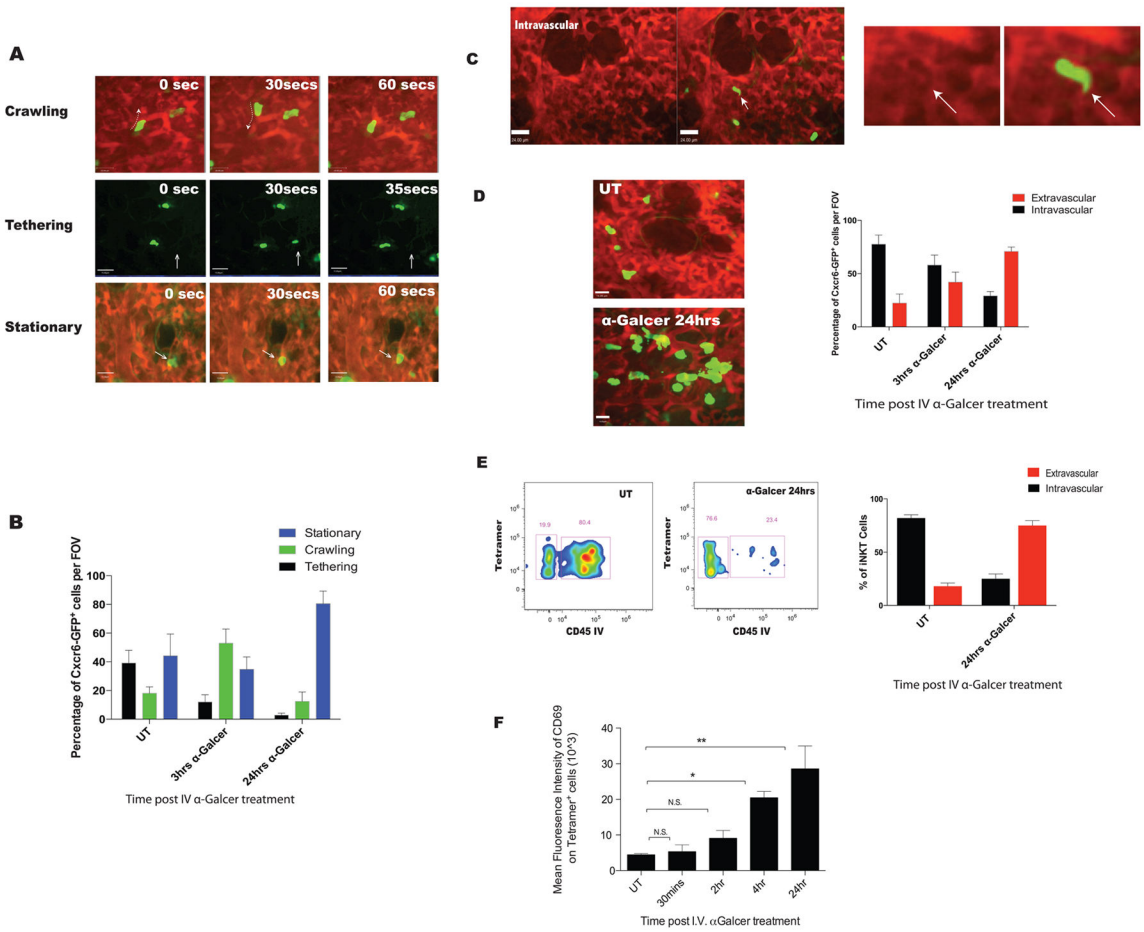

Figure 1. iNKT cells reside predominately in the lung vasculature migrating out upon stimulation with intravenous α-Galcer

A. Three behaviours were observed for CXCR6^{GFP+} cells, identified by IVM in the lungs of untreated mice: (1) Crawling- movement of cells back and forth, (2) tethering- rapid movement of cells with blood flow with short 10–20 second stops and re-entering into blood flow and (3) stationary-cells shows protrusion, slight movement but the cell stays in the general area for 1 mins or longer. Green: CXCR6^{GFP+}; Red: TRITC-dextran. **B.** Quantification of cell behaviors in vehicle treated (UT) or mice treated with 2μg of α-Galcer intravenously. **C.** Localization of cells was assessed using TRITC-dextran shadowing. Arrow indicates shadow formed by CXCR6^{GFP+} cells. **D.** Localization of CXCR6^{GFP+} cells was assessed in naïve mice (UT) or mice treated with treated with 2ug of α-Galcer intravenously. Extravascular CXCR6^{GFP+} take on a larger rounded phenotype and do not display shadows. **E.** Flow cytometry was used to assess cell localization of CD1d tetramer positive cells. “CD45 IV” are indicative of cells that are intravascular. Low to negative CD45 IV is indicative of extravascular localization. **F.** Dynamics of pulmonary iNKT cell activation based on mean fluorescence intensity of CD69 staining on tetramer positive cells after intravenous α-Galcer treatment. Error bars represent standard error of mean. ‘*’ and ‘**’ represent $P < 0.05$ and $P<0.01$, respectively. N = 3–5 animals per group.

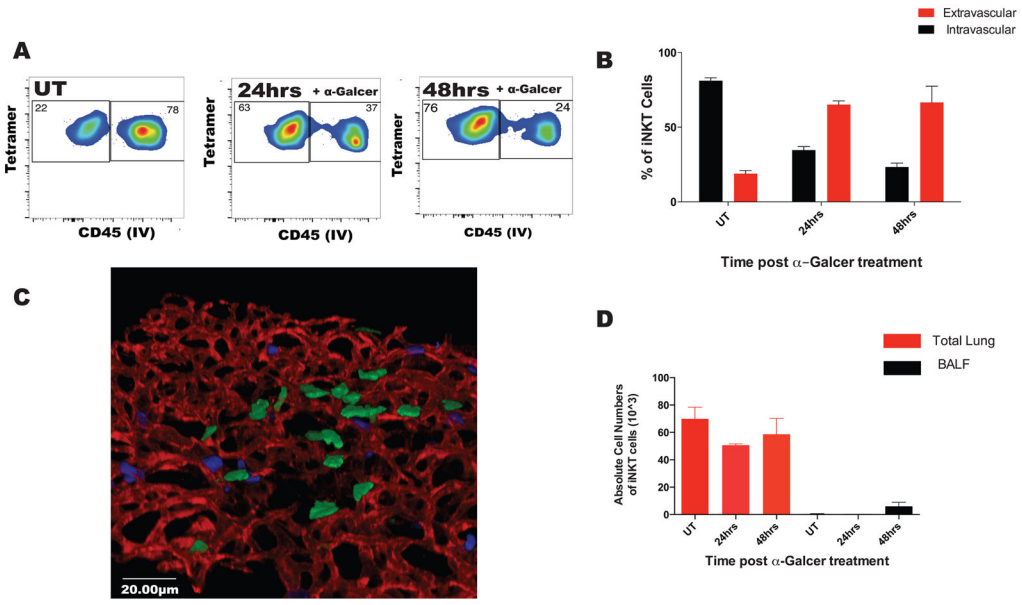

Figure 2. iNKT cells predominately migrate to the interstitial space after intratracheal glycolipid stimulation

A. Mice were treated with aerosolized (400ng) α-Galcer. iNKT cell localization was analyzed by flow cytometry using anti-CD45 i.v injection. **B.** Localization of iNKT was quantified as in (**1E**). **C.** Lungs of mice treated for 48 hours with aerosolized α-Galcer were removed and whole mount staining was performed. 3D reconstruction was performed to assess spatial localization of $CCXR6^{GFP+}$ cells after treatment. Green: $CXCR6^{GFP+}$ cells; Red: CD31 stained endothelial cell; Blue: Ly6G stained neutrophils. **D.** The absolute cell counts for iNKT cells in the total lung homogenate and the bronchial-alveolar lavage fluid, BALF. Error bars represent standard error of mean. N = 3–5 animals per group.

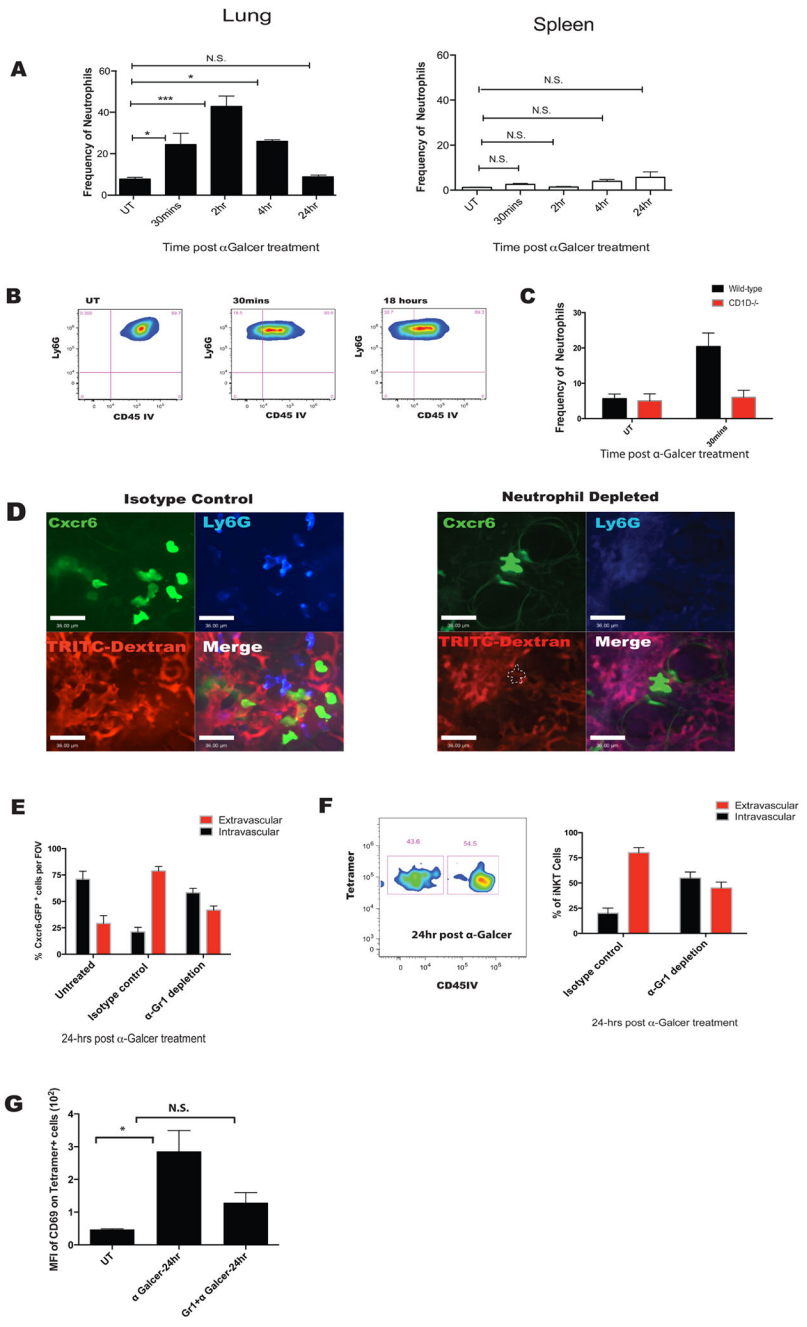

Figure 3. α-Galcer treatment results in an early influx of neutrophils that are necessary for iNKT cell migration out of the vasculature

A. Flow cytometry was utilized to determine dynamics of neutrophil influx in the lung and spleen post i.v. α-Galcer treatment. Graphs represent frequency of neutrophils as a percentage of $CD45^+$ cells. **B.** Extravasation of neutrophils post α-Galcer treatment as in (**1E**). **C.** Quantification of neutrophil percentages in total lung homogenate of CD1dKO mice and wild-type littermates. **D**. Representative IVM images after 24 hours of α-Galcer treatment in istoype control and neutrophil depleted mice. Cell types are labeled respectively. White dotted line defines the shadow left by $CXC6^{GFP+}$ cells on TRITC-

dextran channel. **E.** Quantification of IVM images in (**D**). **F.** iNKT cell localization measured using anti-CD45 infusion in neutrophil depleted and isotype treated mice after i.v. α-Galcer treatment. **G.** iNKT cell activation status measured using CD69 expression in neutrophil depleted or isotype treated mice after i.v. α-Galcer treatment. Error bars represent standard error of mean. '*' represents $P < 0.05$. N = 3–5 animals per group.

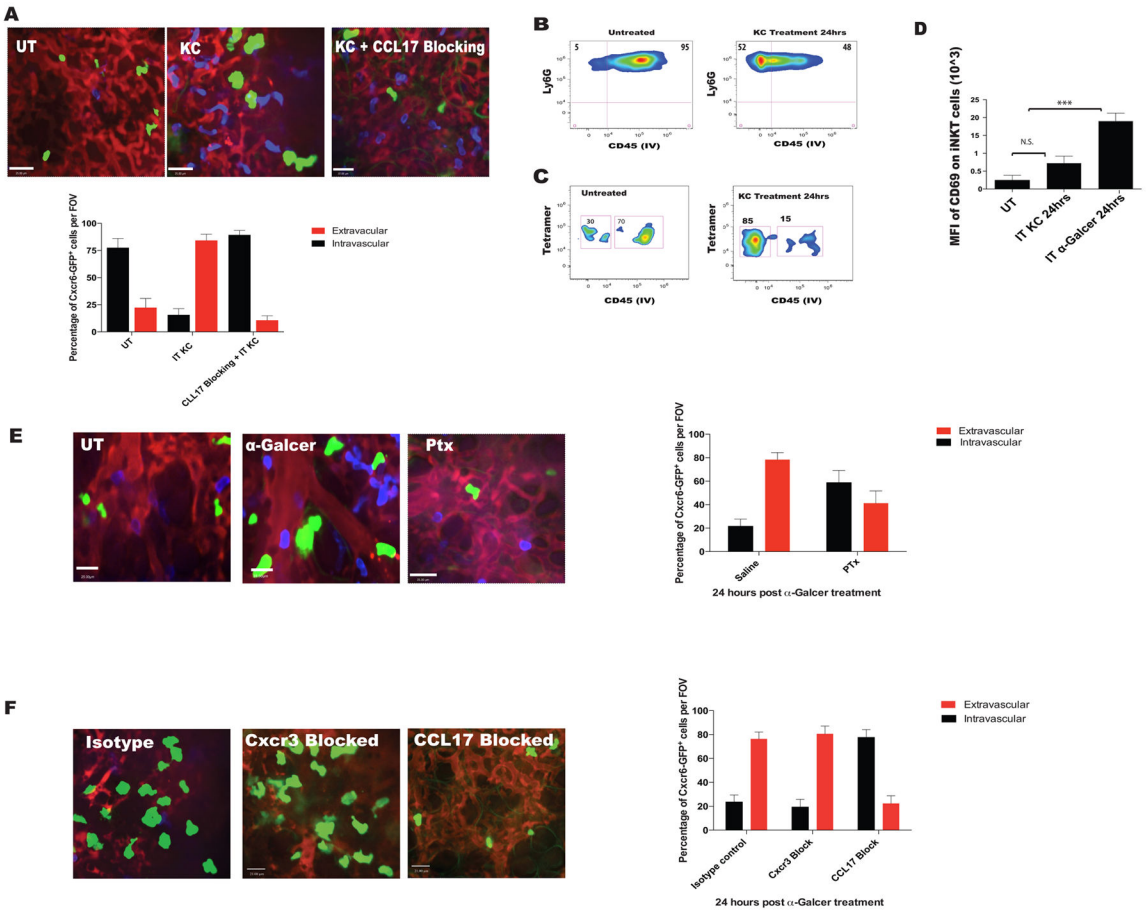

Figure 4. Pulmonary iNKT cell extravasate to the lung interstium in a neutrophil and CCL17 chemokine dependent manner

A. IVM images and quantification of CXC6^{GFP+} cell localization based shadowing technique. Mice were treated with aerosolized KC (200ng) only or intraperitoneal CCL17 neutralizing antibody 30 minutes prior to KC. **B and C.** Neutrophil and iNKT cell localization based on CD45 IV staining after KC administration as in (**1E**). **D.** Mean fluorescence intensity of CD69 on tetramer^{+} iNKT cells after treatment with aerosolized KC; α-Galcer treatment (aerosolized) served as positive control. **E.** IVM was used to assess and quantify pulmonary CXCR6^{GFP+} cell localization in mice pretreated with pertussis toxin or saline control followed by i.v. α-Galcer for 15–24 hours. **F.** IVM was used to assess and quantify pulmonary CXCR6^{GFP+} cell localization in mice pretreated with CCL17 neutralizing antibody, or anti-CXCR3 antibodies, or isotype control followed by i.v. α-Galcer for 15–24 hours. Error bars represent standard error of mean. '***' represent P<0.005. N = 3–5 animals per group.

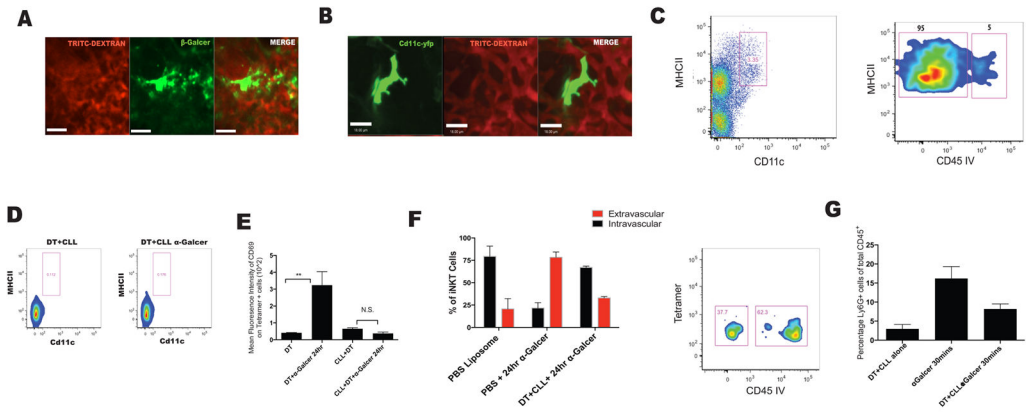

Figure 5. Dendritic cells residing in an extravascular position are the major cell type to take up α-Galcer and are crucial to iNKT cell activation

A. Mice were injected i.v with the probe β-Galcer for 12–18 hours prior to imaging. IVM image of a β-Galcer^{+} cell. **B**. IVM image of a CD11c^{+} DC in the lung. **C.** Flow cytometry and anti-CD45 infusion was used to determine localization of CD11c^{+} MHCII^{hi} cells. **D.** CD11c-DTR mice were depleted of monocytes and CD11c^{+} DCs using i.v administration of CLL (200μL) and intraperitoneal administration of DT 24 hours prior to α-Galcer treatment. **E.** Activation level of iNKT cells was assessed based on mean fluorescence intensity of CD69 on tetramer positive cells. **F.** Localization of iNKT cells based on CD45 IV staining as in (**1E**). **G.** Neutrophil influx in the lung 30 minutes after α-Galcer treatment in mice depleted of monocytes and dendritic cells. Error bars represent standard error of mean. '**' represents P<0.01. N = 3–5 animals per group.

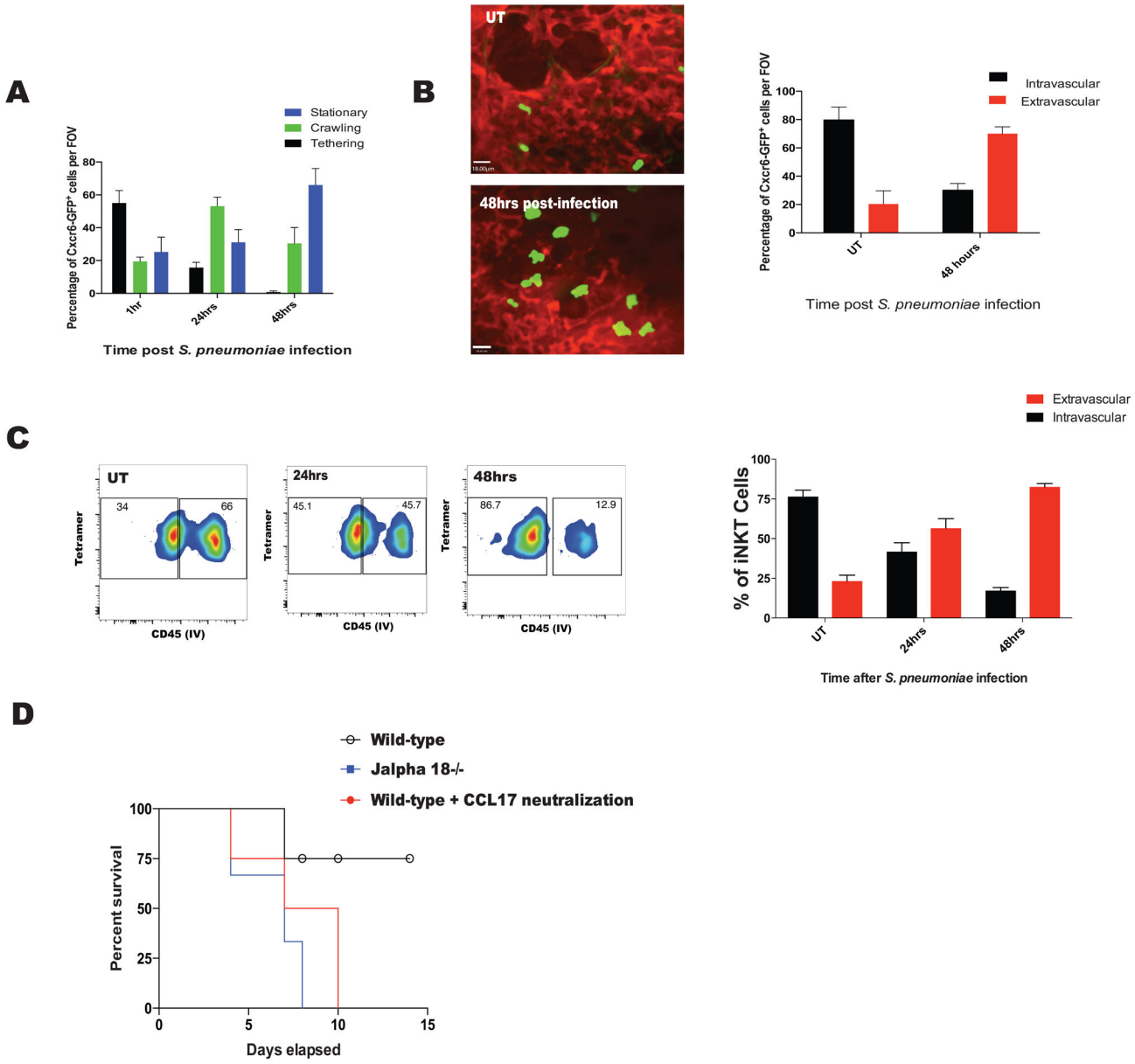

Figure 6. iNKT cell behaviour after *S. pneumoniae* infections emulates that observed after α-Galcer treatment. CCL17 signaling is crucial for survival against *S. pneumoniae* infections

A. Quantification of CXCR6^{GFP+} iNKT cell behavior after aerosolized *S.pneumoniae* using IVM. **B.** Quantification of CXCR6^{GFP+} iNKT cell localization based on IVM and TRITC-dextran shadowing in mice infected with *S.pneumoniae*. **C.** Quantification of iNKT cell localization after *S.pneumoniae* based on CD45 IV staining and flow cytometry. **D.** Survival analysis of mice treated with CCL17 neutralizing antibody. Survival was a significantly different between CCL17 treated mice and control mice based on Mantel-Cox test ($p = 0.006$). Error bars represent standard error of mean. N = 3–5 animals per group.

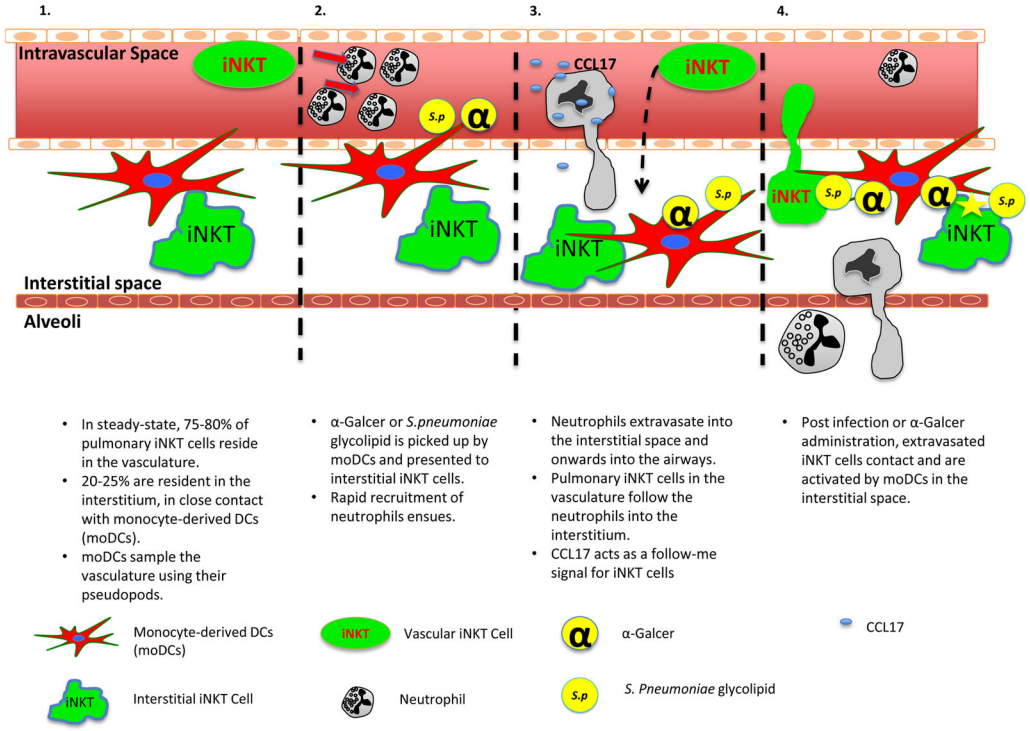

Figure 7. Working model of pulmonary iNKT cell behavior during steady-state and upon activation

In steady-state conditions 75–80% of pulmonary iNKT cells reside in the vasculature, patrolling it; 20–25% of pulmonary iNKT cells reside in the lung interstitial space. Ninety-five percent of DCs, both conventional and monocyte-derived DCs (moDCs), also reside outside the lung vasculature (Panel 1). moDCs, in steady-state, sampled the lung vasculature with their pseudopods. During infections, moDCs capture antigens in the vasculature, such as α-Galcer or S.pneumoniae derived glycolipid, and present these antigens to interstitial iNKT cells. This induces a robust increase in neutrophil recruitment into the lungs (Panel 2). Neutrophils extravasate out of the vasculature into the interstitium and further migrate into the airways. Vascular iNKT cells follow the neutrophils into the interstitium in a CCL17 dependent manner (Panel 3). Once in the interstitium, extravasated iNKT cells come in contact with moDCs and cease further migration out into the airways. There, the iNKT cells become fully activated and assist in clearance of infections (Panel 4).